

## Electronic Structure

Deutsche Ausgabe: DOI: 10.1002/ange.201509430  
Internationale Ausgabe: DOI: 10.1002/anie.201509430

## A Highly Oxidized Cobalt Porphyrin Dimer: Spin Coupling and Stabilization of the Four-Electron Oxidation Product

Soumyajit Dey, Debangsu Sil, and Sankar Prasad Rath\*

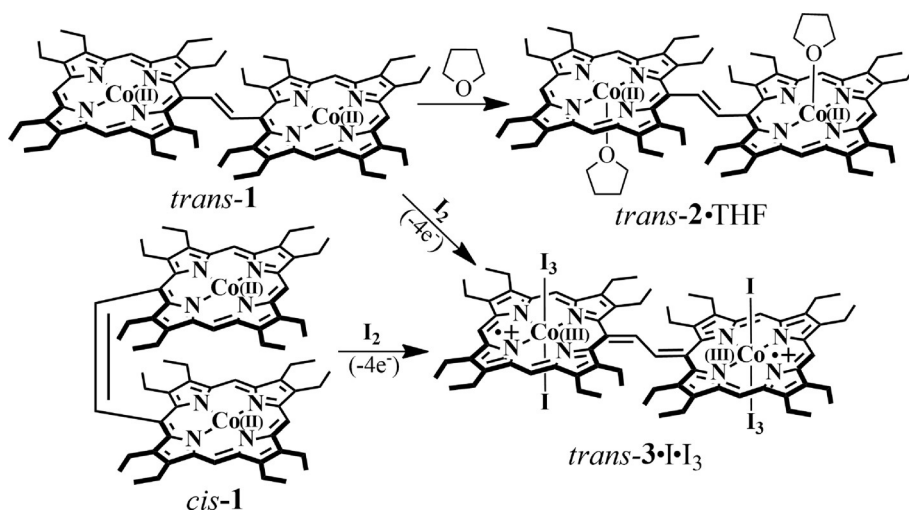
**Abstract:** A highly oxidized cobalt porphyrin dimer is reported. Each cobalt(II) ion and porphyrin ring underwent 1e oxidation with iodine as the oxidant to give a 4e-oxidized cobalt(III) porphyrin  $\pi$ -cation radical dimer. The bridging ethylene group allows for substantial conjugation of the porphyrin macrocycles, thus leading to a strong antiferromagnetic coupling between the  $\pi$ -cation radicals and to stabilization of the singlet state. X-ray crystallography clearly showed that the complex may be considered as a real supramolecule rather than two cobalt(III) porphyrin  $\pi$ -cation radicals that interact through space.

Highly oxidized metalloporphyrins have been identified as intermediates in a number of heme proteins, including catalase, peroxidase, and cytochrome P-450.<sup>[1,2]</sup> The biological significance, unusual electronic properties, and unique reactivities of these intermediates have generated much interest. However, comprehensive characterization and mechanistic studies are hindered by their intrinsic reactivity and lability. In this context, synthetic metalloporphyrin  $\pi$ -cation radicals ( $MP^{\bullet+}$ ) serve as models for these transient species.<sup>[3–6]</sup> In synthetic metalloporphyrin  $\pi$ -cation radicals of first-row transition metals, cobalt has common oxidation states of +2 and +3, as does iron.<sup>[7,8]</sup> Furthermore, like the hemes, cobaltous porphyrins can readily lose one electron from each metal center and porphyrin macrocycle to form  $Co^{III}$   $\pi$ -cation radicals (2e oxidation).<sup>[7]</sup>

A large number of diheme enzymes, such as MauG<sup>[9]</sup> and bacterial diheme cytochrome c peroxidases (bCcP),<sup>[10]</sup> are known to catalyze various chemical transformations in biology. A tryptophan residue located halfway between the heme centers has been postulated to act as a bridge in the electronic communication between two heme centers.<sup>[9,10]</sup> A hole-hopping mechanism has been suggested

in which the tryptophan residue undergoes reversible oxidation and reduction to increase the effective electronic coupling and escalate the rate of reversible electron transfer among the heme groups in bis-Fe<sup>IV</sup> MauG.<sup>[9]</sup> However, the electronic coupling between porphyrin macrocycles, in the ground and/or excited state, can also be facilitated by covalently attached linkers.<sup>[11,12]</sup> In the present study, we used cobalt porphyrin dimers in which two porphyrin macrocycles are covalently connected through an ethylene bridge and explored the effect of the bridge in communicating between two highly oxidized cobalt porphyrins.

The treatment of a cobalt(II) porphyrin with iodine is known to generate either a cobalt(III) porphyrin or a cobalt(II) porphyrin  $\pi$ -cation radical; some of these species have also been structurally characterized.<sup>[7a,c,11c]</sup> However, the oxidation of both the metal and porphyrin centers with iodine has not been reported so far. Herein, we report the structure and properties of a 4e-oxidized cobalt porphyrin dimer in which both the metal and the porphyrin centers have been oxidized by iodine. The ethylene spacer enables electronic communication between two oxidized segments to make the system fully conjugated and thereby stabilized.



Scheme 1. Synthesis of the complexes.

[\*] S. Dey, D. Sil, Prof. Dr. S. P. Rath  
Department of Chemistry, Indian Institute of Technology Kanpur  
Kanpur-208016 (India)  
E-mail: sprath@iitk.ac.in

Supporting information for this article is available on the WWW under <http://dx.doi.org/10.1002/anie.201509430>.

The ethene-bridged cobalt(II) porphyrin dimers *trans*-1 and *cis*-1 (Scheme 1) were synthesized in excellent yield by heating the corresponding free ligand with  $Co(OAc)_2$  (added as a solution in methanol) in  $CH_2Cl_2$  at reflux under  $N_2$ . The dissolution of *trans*-1 into THF resulted in the formation of the five-coordinate complex *trans*-2·THF, which was isolated

as a solid and structurally characterized. The gradual addition of iodine to *cis*-**1** in CH<sub>2</sub>Cl<sub>2</sub> resulted in a steep decrease in the intensity of the Soret band at 386 nm, along with the appearance of a new band at 511 nm and two broad bands at 740 and 1240 nm (Figure 1). The oxidized product, *trans*-

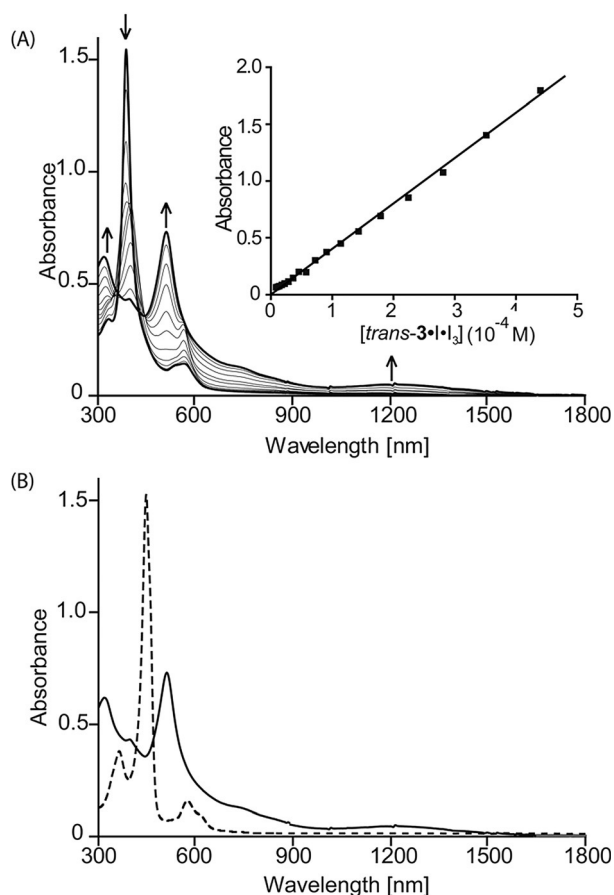


**Figure 1.** A) Change in the UV/Vis/NIR spectrum (in CH<sub>2</sub>Cl<sub>2</sub> at 295 K) of *cis*-**1** ( $5 \times 10^{-6}$  M) upon the gradual addition of I<sub>2</sub>. Inset: Change in the absorption spectrum of *trans*-**3-I-I**<sub>3</sub> at 1240 nm as a function of concentration. B) UV/Vis/NIR spectra (in CH<sub>2</sub>Cl<sub>2</sub> at 295 K) of 1,2-bis[iodocobalt(III)-5-(2,3,7,8,12,13,17,18-octaethylporphyrinyl)]ethane<sup>[11c]</sup> (dotted line) and *trans*-**3-I-I**<sub>3</sub> (solid line).

**3-I-I**<sub>3</sub>, was also isolated in the solid state in good yield and structurally characterized. The addition of iodine to *trans*-**1** led to a similar spectral change and generated the same oxidized product *trans*-**3-I-I**<sub>3</sub> (see Figure S1 in the Supporting Information). The broad NIR band centered at 1240 nm can be attributed to charge-resonance (CR)<sup>[13]</sup> stabilization in the binuclear dicationic diradical complex, and its intensity was found to be linearly correlated with the concentration of *trans*-**3-I-I**<sub>3</sub> (Figure 1 A; see also Figure S2) which supports the intramolecular origin of the band. Interestingly, however, similar oxidation of the ethane-bridged cobalt(II) porphyrin dimer with I<sub>2</sub> only produced the corresponding five-coordinate Co<sup>III</sup> complex with axial iodide coordination (see Scheme S1 in the Supporting Information), for which no absorption maxima around 500, 750, and 1200 nm were observed (Figure 1 B; see also Figures S3 and S4).<sup>[11c]</sup> Thus,

the bands observed at 511, 740, and 1240 nm for *trans*-**3-I-I**<sub>3</sub> are attributed to the extensive conjugation between the two Co<sup>III</sup>-porphyrin  $\pi$ -cation radicals.

The characteristics of the electronic spectrum of a typical porphyrin  $\pi$ -cation radical as compared to that of the unoxidized complex are a new low-energy band and a dramatically broadened, blue-shifted Soret band.<sup>[6]</sup> All the characteristic features of  $\pi$ -cation-radical formation were observed for *trans*-**3-I-I**<sub>3</sub>. The drastic reduction of the Soret band intensity in *trans*-**3-I-I**<sub>3</sub> (Figure 1) also suggests that the aromaticity of the porphyrin rings in the complex is decreased, which, however, facilitates the extensive conjugation through the bridge. FTIR spectroscopy is an important tool for the identification of porphyrin  $\pi$ -cation radicals. The porphyrin dimer *trans*-**3-I-I**<sub>3</sub> showed characteristic C $\alpha$ –C $\text{meso}$  and C $\beta$ –C $\beta$  stretching frequencies at 1560 and 1615 cm<sup>-1</sup>, respectively (see Figure S5), which suggests the formation of porphyrin  $\pi$ -cation radical in the complex.<sup>[6,14]</sup>

Dark-red crystals<sup>[15]</sup> of *trans*-**2-THF** were grown by the slow diffusion of *n*-hexane into a solution of *trans*-**1** in THF at room temperature in air. The complex crystallizes in the triclinic crystal system with the *P* $\bar{1}$  space group. The molecular structure of the complex (see Tables S1 and S2 in the Supporting Information) is depicted in Figure 2 (see Fig-

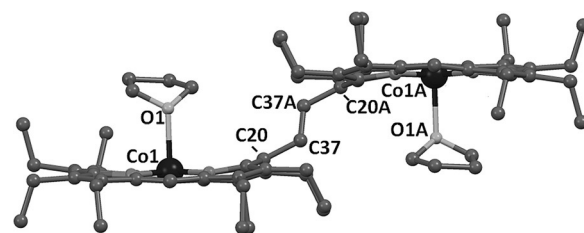


**Figure 2.** Molecular structure (at 100 K) of *trans*-**2-THF** (H atoms have been omitted for clarity). Selected bond distances [Å] and angles [°]: Co1–N1 1.977(3), Co1–N2 1.975(2), Co1–N3 1.975(3), Co1–N4 1.970(2), Co1–O1 2.273(2), C20–C37 1.500(4), C37–C37A 1.302(6); N1–Co1–N2 90.98(10), N1–Co1–N3 175.16(11), N1–Co1–N4 94.44(10), N2–Co1–N3 89.12(10), N2–Co1–N4 173.55(11), N3–Co1–N4 90.75(10); N1–Co1–O1 91.40(9), N2–Co1–O1 92.01(10), N3–Co1–O1 93.43(10), N4–Co1–O1 94.44(10).

ure S6 for the molecular packing). The Co<sup>II</sup> centers adopt a square-pyramidal geometry in which the N–Co–N and N–Co–O bond angles are close to 90°. The Co–N<sub>p</sub> and Co–O (THF) distances were found to be slightly longer than those of the ethane-bridged analogue, 1,2-bis[tetrahydrofuranocobalt(II)-5-(2,3,7,8,12,13,17,18-octaethylporphyrinyl)]ethane.<sup>[11c]</sup> Also, the THF rings are significantly bent in the complex. They lie nearly parallel to the porphyrin ring associated with the same cobalt center, thus allowing efficient CH– $\pi$  interactions between the THF and porphyrin moieties.

Dark-brown crystals<sup>[15]</sup> of *trans*-**3-I-I**<sub>3</sub> were grown by the slow diffusion of *n*-hexane into a solution in benzene of a mixture of *cis*-**1** and iodine in a 1: > 4 molar ratio at room temperature in air. The molecule crystallizes in the monoclinic crystal system with the *P*2<sub>1</sub>/*c* space group. The X-ray crystal structure is shown in Figure 3 A (see Figure S7 for the molecular packing). Each Co<sup>III</sup> center adopts a six-coordinate

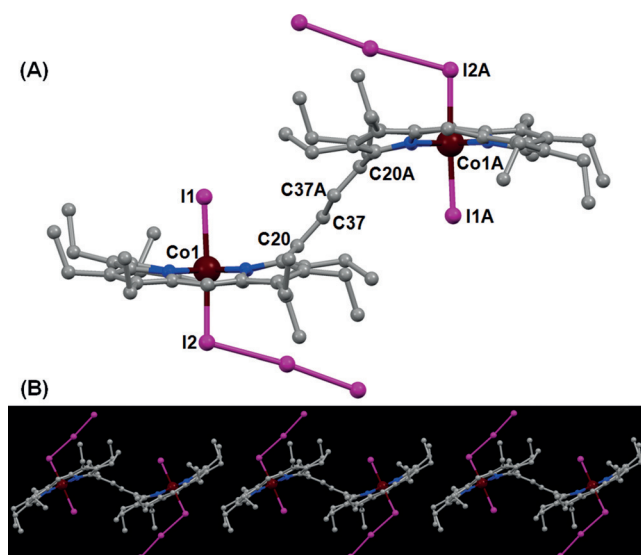


**Figure 3.** A) Molecular structure (at 100 K) of *trans*-3-I-I<sub>3</sub> (H atoms have been omitted for clarity). Selected bond distances [Å] and angles [°]: Co1–N1 1.943(7), Co1–N2 1.947(7), Co1–N3 1.935(7), Co1–N4 1.981(7), Co1–I1 2.5909(13), Co1–I2 2.6030(13), C20–C37 1.381(12), C37–C37A 1.392(17); N1–Co1–N2 90.5(3), N1–Co1–N3 178.7(3), N1–Co1–N4 88.9(3), N2–Co1–N3 90.7(3), N2–Co1–N4 177.0(3), N3–Co1–N4 89.8(3), N1–Co1–I1 90.0(2), N2–Co1–I1 90.1(2), N3–Co1–I1 90.4(2), N4–Co1–I1 92.9(2), N1–Co1–I2 90.3(2), N2–Co1–I2 87.0(2), N3–Co1–I2 89.3(2), N4–Co1–I2 90.1(2). B) Diagram showing the molecular arrangement in the crystal lattice.

octahedral geometry with iodide and triiodide as axial ligands, and the metal is displaced towards I<sup>−</sup> by 0.08 Å from the least-squares plane of the C<sub>20</sub>N<sub>4</sub> porphyrinato core. The average Co–N<sub>p</sub> bond distance was found to be 1.951(7) Å, which falls within the observed range for cobalt(III) porphyrinate-s<sup>[7a,c,8,11c]</sup> but is longer than that of five-coordinate 1,2-bis[iodocobalt(III)-5-(2,3,7,8,12,13,17,18-octaethylporphyrinyl)]ethane.<sup>[11c]</sup> To the best of our knowledge, no structure of a cobalt(III) porphyrin  $\pi$ -cation radical has been reported previously.

The salient structural features of the complexes reported herein are compared in Table 1 along with those reported earlier for *cis*-1.<sup>[16]</sup> The average interplanar angle ( $\alpha$ ) between the least-squares planes of the C<sub>20</sub>N<sub>4</sub> porphyrinato cores and the C<sub>4</sub> plane of the bridging ethylene group is 60.5° in *cis*-1, 71.7° in *trans*-2·THF, and 49.0° in *trans*-3-I-I<sub>3</sub>. The smaller angle  $\alpha$  in *trans*-3-I-I<sub>3</sub> favors the electronic communication between the two porphyrin  $\pi$ -cation radicals through the

**Table 1:** Selected geometrical parameters.

	<i>cis</i> -1 <sup>[a]</sup>		<i>trans</i> -2·THF	<i>trans</i> -3-I-I <sub>3</sub>
	core I	core II		
Co–N <sub>p</sub> <sup>[b]</sup>	1.971(5)	1.951(5)	1.974(3)	1.951(7)
Co–O/I <sup>[b]</sup>	–	–	2.273(2)	2.5909(13)
Co–I(I <sub>3</sub> ) <sup>[b]</sup>	–	–	–	2.6030(13)
C20–C37 <sup>[b]</sup>	1.504(5)	1.500(5)	1.500(4)	1.381(12)
C37–C37A <sup>[b]</sup>	1.332(5)	–	1.302(6)	1.392(17)
$\alpha$ <sup>[c]</sup>	64.5	56.5	71.7	49.0

[a] Taken from Ref. [16]. [b] Average value in Å. [c] Inter-planar angle (in degrees) between the least-squares plane of the C<sub>20</sub>N<sub>4</sub> porphyrinato core and the C<sub>4</sub> plane of the bridging ethylene group (see Figure S8).

bridging ethylene group, thus leading to a change in the C20–C37 and C37–C37A bond distances. The average C20–C37 and C37–C37A distances were found to be 1.502(5) and 1.332(5) Å, respectively, in *cis*-1, and 1.500(4) and 1.302(6) Å in *trans*-2·THF (Table 1). In sharp contrast, the C20–C37 and C37–C37A bond distances in *trans*-3-I-I<sub>3</sub> are 1.381(12) and 1.392(17) Å, respectively. Thus, the linker between the porphyrin rings no longer resembles an ethylene bridge (C–CH=CH–C), but instead it is as if *exo*-methylene groups on the two porphyrin rings were connected to one another (C=CH–CH=C). This structure is indicative of the strong  $\pi$ -conjugation between the two cation radicals in the complex. The electrostatic repulsion between the two porphyrin  $\pi$ -cation radicals in the oxidized complex along with the steric repulsion arising from axial ligand coordination have forced the two porphyrin macrocycles to be separated as far as possible from one another (*trans* isomer) through facile C–C bond rotation in the bridge, which results in the conversion of the *cis* isomer into the *trans* isomer. In fact, oxidation leads to a change in the identity of the bridge from ethylene to *exo*-methylene and thereby facilitates this transformation.

Iodine is known to be a mild oxidant. Saddle-shaped Co<sup>II</sup>[OET(*p*-R)PP] (in which R = CF<sub>3</sub>, H, CH<sub>3</sub> and OETPP is the dianion of 2,3,7,8,12,13,17,18-octaethyl-5,10,15,20-tetra-phenylporphyrinato) is readily oxidized with I<sub>2</sub> to the corresponding 1e-oxidized complex Co[OET(*p*-R)PP]I with a clear indication of the formation of a porphyrin  $\pi$ -cation radical.<sup>[7a]</sup> Also, the oxidation of (tetrabenzoporphyrinato)cobalt(II), Co(tbp), with iodine yielded a cobalt(II) porphyrin  $\pi$ -cation radical, Co(tbp)<sup>•</sup>I, with iodide as the counter anion.<sup>[7c]</sup> A highly oxidized cobalt complex of octaethylbilindione, an open-chain tetrapyrrole ligand, was found to be stabilized in the form of its triiodide salt.<sup>[17]</sup> However, the addition of I<sub>2</sub> to the ethane-bridged cobalt(II) porphyrin dimer resulted in the formation of a five-coordinate complex in which Co<sup>II</sup> was oxidized to Co<sup>III</sup> with an axial iodide ligand.<sup>[11c]</sup> In sharp contrast, the ethylene-bridged cobalt(II) porphyrin dimers *trans*-1 and *cis*-1 were readily oxidized by iodine to generate the cobalt(III) porphyrin  $\pi$ -cation radical dimer *trans*-3-I-I<sub>3</sub>. Both the metal and the porphyrin centers are oxidized in this complex, and the ethylene spacer enables strong  $\pi$ -electronic communication between the two oxidized segments to generate a fully delocalized system. An electrochemical study of *trans*-3-I-I<sub>3</sub> at 295 K under nitrogen in CH<sub>2</sub>Cl<sub>2</sub> with 0.1M tetrabutylammonium hexafluorophosphate (TBAHFP) as the supporting electrolyte showed two irreversible redox couples at +0.20 and −0.16 V (vs. Ag/AgCl) (see Figure S9), which clearly justify the stabilization of such an oxidized complex.

The solid-state structure is preserved in solution, as reflected by <sup>1</sup>H NMR spectroscopy. Figure 4 shows the well-resolved spectra of *cis*-1 and *trans*-3-I-I<sub>3</sub>. The <sup>1</sup>H NMR spectrum of *cis*-1 in CDCl<sub>3</sub> (Figure 4, trace A) shows the characteristic paramagnetic shifts and peak broadening expected for a low-spin cobalt(II) porphyrin complex. The eight methylene proton resonances and two well-separated *meso* signals with a 1:2 intensity ratio are indicative of the cofacial orientation (*cis*) of the two porphyrin macrocycles.<sup>[11c,16]</sup> However, upon oxidation by iodine, all the



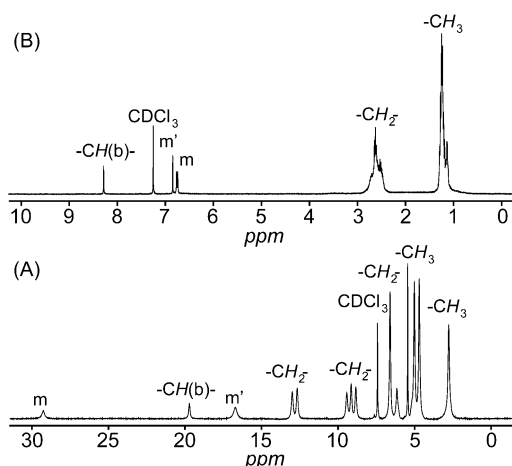


Figure 4.  $^1\text{H}$  NMR spectra (295 K,  $\text{CDCl}_3$ ) of A) *cis*-1 and B) *trans*-3-I-I<sub>3</sub>.

resonances are shifted upfield and thereby moved into the diamagnetic region in *trans*-3-I-I<sub>3</sub> (Figure 4, trace B). The two *meso* signals that were earlier well-separated in *cis*-1 (trace A) are now almost on the top of each other (trace B), which suggests the stabilization of the *trans* form in *trans*-3-I-I<sub>3</sub>. The upfield shifting of the *meso* resonances in *trans*-3-I-I<sub>3</sub> is consistent with the reduced aromaticity in the porphyrin moiety as a result of the formation of  $\pi$ -cation radicals.<sup>[18]</sup> However, the sharpness and position of the proton signals suggest the diamagnetic nature of the complex owing to strong antiferromagnetic coupling between two unpaired radical spins.

The inter-ring coupling between two porphyrin  $\pi$ -cation radicals has been shown to be closely related to the degree of porphyrin-ring overlap in four- and five-coordinate complexes.<sup>[6,19]</sup> For example, the  $[\text{Zn}(\text{OEP}^*)(\text{OH}_2)]^+$  cation ( $\text{H}_2\text{OEP}$  = octaethylporphyrin) forms a strongly interacting dimer  $[[\text{Zn}(\text{OEP}^*)(\text{OH}_2)]_2]^{2+}$ , in which the two cores are completely overlapped with a short interplanar separation of 3.31 Å; as a result, the unpaired electrons are so strongly coupled that the molecule is diamagnetic.<sup>[19a,b]</sup> A similar situation was observed for  $[\text{Mg}(\text{OEP}^*)]^+$ .<sup>[19c]</sup> Owing to the six-coordinate nature of *trans*-3-I-I<sub>3</sub>, both the inter- and intramolecular separation between the two porphyrin macrocycles are substantially larger (see Figure S7). However, both porphyrin  $\pi$ -cation radicals exhibit substantial intramolecular conjugation through the bridging ethylene group in a closed-shell system, which results in the formation of a diamagnetic complex, *trans*-3-I-I<sub>3</sub>.

We carried out computational studies by using DFT at the UB3LYP/LanL2DZ/3-21G level to gain more insight into the electronic structure. The optimized geometries of *trans*-3-I-I<sub>3</sub> are shown in Figure 5A for two possible combinations of spins in a closed-shell system: singlet (considering an antiferromagnetic interaction between two porphyrin  $\pi$ -cation radical spins) and triplet states (considering a ferromagnetic interaction between two porphyrin  $\pi$ -cation radical spins). Most importantly, the calculation based on the singlet state virtually reproduces the change in the C20–C37 and C37–C37A bond distances of the bridge as observed in the X-ray crystal structure of the complex (Figure 3). Furthermore,

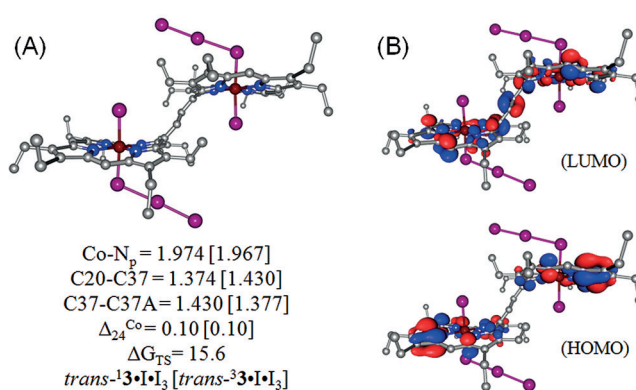


Figure 5. A) UB3LYP optimized geometries of *trans*-1,3-I-I<sub>3</sub>, as obtained by using the LanL2DZ basis set for cobalt and 3-21G for all other atoms, with bond lengths in Å.  $\Delta_{24}^{\text{Co}}$  is the average displacement (in Å) of the metal from the least-squares plane of the  $\text{C}_{20}\text{N}_4$  porphyrinato core.  $\Delta G_{\text{TS}}$  is given relative to the singlet spin state in  $\text{kcal mol}^{-1}$  (including ZPE). B) HOMO and LUMO of *trans*-1,3-I-I<sub>3</sub>.

comparison of the relative energies of *trans*-3-I-I<sub>3</sub> (see Figure S10), obtained by three different modes of calculation, suggest the relative stabilization of the singlet spin state over the triplet state by 15.6  $\text{kcal mol}^{-1}$  (including the zero-point energy, ZPE). The LUMO of *trans*-3-I-I<sub>3</sub> for the singlet spin state (Figure 5B) was found to have significant coefficients on the bridging ethylene group, thus suggesting strong  $\pi$  conjugation of the unpaired spins through the bridge; this result is also in good agreement with our experimental results.

In summary, we have presented herein the synthesis, structure, and properties of a 4e-oxidized cobalt porphyrin dimer, in which each metal center and porphyrin ring has undergone 1e oxidation with iodine. This oxidation also facilitated the facile conversion of the *cis* isomer into the *trans* isomer. Each  $\text{Co}^{\text{III}}$  center adopts a six-coordinate octahedral geometry in the oxidized complex, with iodide and triiodide as axial ligands. In sharp contrast, similar oxidation of the ethane-bridged analogue by  $\text{I}_2$  resulted in the formation of a five-coordinate complex, in which  $\text{Co}^{\text{II}}$  had been oxidized to  $\text{Co}^{\text{III}}$ . Through the ethylene bridge both cobalt(III) porphyrin  $\pi$ -cation radicals exhibited substantial conjugation, thus leading to strong antiferromagnetic coupling, which stabilized the singlet state. The conversion of the ethylene bridge to an “exo-methylene” connection emphasizes the pivotal role of the bridge in the electronic communication. The oxidized complex reported herein has very unusual spectral and geometrical features and can be viewed as a single supra-molecular unit instead of two interacting cobalt(III) porphyrin  $\pi$ -cation radicals. Computational calculations clearly supported the experimental results.

## Acknowledgements

S.P.R., S.D., and D.S. thank the Science and Engineering Research Board (SERB), New Delhi and the Council of Scientific and Industrial Research (CSIR), New Delhi for financial support and IIT Kanpur for the infrastructure. S.D. and D.S. thank UGC for their fellowships.

**Keywords:** antiferromagnetic coupling · cobalt · oxidation ·  $\pi$ -cation radicals · porphyrin dimers

**How to cite:** *Angew. Chem. Int. Ed.* **2016**, *55*, 996–1000  
*Angew. Chem.* **2016**, *128*, 1008–1012

- [1] a) T. L. Poulos, *Chem. Rev.* **2014**, *114*, 3919–3962; b) M. Alfonso-Prieto, X. Biarnés, P. Vidossich, C. Rovira, *J. Am. Chem. Soc.* **2009**, *131*, 11751–11761.
- [2] a) A. B. McQuarters, M. W. Wolf, A. P. Hunt, N. Lehnert, *Angew. Chem. Int. Ed.* **2014**, *53*, 4750–4752; *Angew. Chem.* **2014**, *126*, 4846–4848; b) J. Rittler, M. T. Green, *Science* **2010**, *330*, 933–937; c) W. Nam, *Acc. Chem. Res.* **2007**, *40*, 522–531; d) I. G. Denisov, T. M. Makris, S. G. Sligar, I. Schlichting, *Chem. Rev.* **2005**, *105*, 2253–2277; e) S. Shaik, D. Kumar, S. P. de Visser, A. Altun, W. Thiel, *Chem. Rev.* **2005**, *105*, 2279–2328.
- [3] a) A.-R. Han, Y. J. Jeong, Y. Kang, J. Y. Lee, M. S. Seo, W. Nam, *Chem. Commun.* **2008**, 1076–1078; b) Y. Kang, H. Chen, Y. J. Jeong, W. Lai, E. H. Bae, S. Shaik, W. Nam, *Chem. Eur. J.* **2009**, *15*, 10039–10046.
- [4] a) Z. Cong, T. Kurahashi, H. Fujii, *Angew. Chem. Int. Ed.* **2011**, *50*, 9935–9939; *Angew. Chem.* **2011**, *123*, 10109–10113; b) S. R. Bell, J. T. Groves, *J. Am. Chem. Soc.* **2009**, *131*, 9640–9641.
- [5] a) M. Nakamura, Y. Ohgo, A. Ikezaki, *J. Inorg. Biochem.* **2008**, *102*, 433–445; b) M. Nakamura, *Coord. Chem. Rev.* **2006**, *250*, 2271–2294.
- [6] a) M. Li, T. J. Neal, G. R. A. Wyllie, C. E. Schulz, W. R. Scheidt, *Inorg. Chem.* **2010**, *49*, 8078–8085; b) A. Takai, C. P. Gros, J. M. Barbe, R. Guillard, S. Fukuzumi, *Chem. Eur. J.* **2009**, *15*, 3110–3122; c) M. Li, T. J. Neal, G. R. A. Wyllie, A. G. Oliver, C. E. Schulz, W. R. Scheidt, *Inorg. Chem.* **2011**, *50*, 9114–9121; d) R. J. Cheng, C. H. Ting, T. C. Chao, T.-H. Tseng, P. P.-Y. Chen, *Chem. Commun.* **2014**, *50*, 14265–14268.
- [7] a) R.-J. Cheng, Y.-H. Chen, C.-C. Chen, G.-H. Lee, S.-M. Peng, P. P.-U. Chen, *Inorg. Chem.* **2014**, *53*, 8848–8850; b) M. Satoh, Y. Ohba, S. Yamauchi, M. Iwaizumi, *Inorg. Chem.* **1992**, *31*, 298–303; c) K. Liou, T. P. Newcomb, M. D. Heagy, J. A. Thompson, W. B. Heuer, R. L. Musselman, C. S. Jacobsen, B. M. Hoffman, J. A. Ibers, *Inorg. Chem.* **1992**, *31*, 4517–4523; d) W. A. Oertling, A. Salehi, C. K. Chang, G. T. Babcock, *J. Phys. Chem.* **1989**, *93*, 1311–1319.
- [8] a) J. Li, B. C. Noll, A. G. Oliver, G. Ferraudi, A. G. Lappin, W. R. Scheidt, *Inorg. Chem.* **2010**, *49*, 2398–2406; b) E.-Y. Choi, P. M. Barron, R. W. Novotny, H.-T. Son, C. Hu, W. Choe, *Inorg. Chem.* **2009**, *48*, 426–428; c) J. Goodwin, T. Kurtikyan, J. Standard, R. Walsh, B. Zheng, D. Parmley, J. Howard, S. Green, A. Mardiyukov, D. E. Przybyla, *Inorg. Chem.* **2006**, *45*, 2215–2223; d) H. Sun, V. V. Smirnov, S. G. DiMaggio, *Inorg. Chem.* **2003**, *42*, 6032–6040.
- [9] a) L. M. R. Jensen, R. Sanishvili, V. L. Davidson, C. M. Wilmot, *Science* **2010**, *327*, 1392–1394; b) Y. Wang, M. E. Graichen, A. Liu, A. R. Pearson, C. M. Wilmot, V. L. Davidson, *Biochemistry* **2003**, *42*, 7318–7325.
- [10] a) G. S. Pulcu, K. E. Frato, R. Gupta, H. R. Hsu, G. A. Levine, M. P. Hendrich, S. J. Elliott, *Biochemistry* **2012**, *51*, 974–985; b) J. Seidel, M. Hoffmann, K. E. Ellis, A. Seidel, T. Spatzal, S. Gerhardt, S. J. Elliott, O. Einsle, *Biochemistry* **2012**, *51*, 2747–2756; c) A. Echali, C. F. Goodhew, G. W. Pettigrew, V. Fülöp, *Structure* **2006**, *14*, 107–117.
- [11] a) D. Sil, S. P. Rath, *Dalton Trans.* **2015**, *44*, 16195–16211; b) M. A. Sainna, D. Sil, D. Sahoo, B. Martin, S. P. Rath, P. Comba, S. P. de Visser, *Inorg. Chem.* **2015**, *54*, 1919–1930; c) S. Dey, S. P. Rath, *Dalton Trans.* **2014**, *43*, 2301–2314; d) D. Sil, F. S. T. Khan, S. P. Rath, *Inorg. Chem.* **2014**, *53*, 11925–11936; e) S. Bhowmik, S. Dey, D. Sahoo, S. P. Rath, *Chem. Eur. J.* **2013**, *19*, 13732–13744; f) S. K. Ghosh, S. Bhowmik, D. Sil, S. P. Rath, *Chem. Eur. J.* **2013**, *19*, 17846–17859; g) S. Bhowmik, S. K. Ghosh, S. P. Rath, *Chem. Eur. J.* **2012**, *18*, 13025–13037; h) S. Bhowmik, S. K. Ghosh, S. P. Rath, *Chem. Commun.* **2011**, *47*, 4790–4792; i) S. K. Ghosh, S. P. Rath, *J. Am. Chem. Soc.* **2010**, *132*, 17983–17985; j) S. K. Ghosh, R. Patra, S. P. Rath, *Inorg. Chem.* **2010**, *49*, 3449–3460; k) S. Bhowmik, D. Sil, R. Patra, S. P. Rath, *J. Chem. Sci.* **2011**, *123*, 827–837; l) S. K. Ghosh, R. Patra, S. P. Rath, *Inorg. Chim. Acta* **2010**, *363*, 2791–2799; m) S. K. Ghosh, R. Patra, S. P. Rath, *Inorg. Chem.* **2008**, *47*, 10196–10198.
- [12] a) M. Son, Y. M. Sung, S. Tokui, N. Fukui, H. Yorimitsu, A. Osuka, D. Kim, *Chem. Commun.* **2014**, *50*, 3078–3080; b) L. Rintoul, S. R. Harper, D. P. Arnold, *Phys. Chem. Chem. Phys.* **2013**, *15*, 18951–18964; c) O. Locos, B. Bašić, J. C. McMurtrie, P. Jensen, D. P. Arnold, *Chem. Eur. J.* **2012**, *18*, 5574–5588; d) L. J. Esdaile, P. Jensen, J. C. McMurtrie, D. P. Arnold, *Angew. Chem. Int. Ed.* **2007**, *46*, 2090–2093; *Angew. Chem.* **2007**, *119*, 2136–2139; e) M. J. Frampton, H. Akdas, A. R. Cowley, J. E. Rogers, J. E. Slagle, P. A. Fleitz, M. Drobizhev, A. Rebane, H. L. Anderson, *Org. Lett.* **2005**, *7*, 5365–5368.
- [13] a) J. Geng, I. Davis, A. Liu, *Angew. Chem. Int. Ed.* **2015**, *54*, 3692–3696; *Angew. Chem.* **2015**, *127*, 3763–3767; b) A. Heckmann, C. Lambert, *Angew. Chem. Int. Ed.* **2012**, *51*, 326–392; *Angew. Chem.* **2012**, *124*, 334–404; c) D. L. Sun, S. V. Rosokha, S. V. Lindeman, J. K. Kochi, *J. Am. Chem. Soc.* **2003**, *125*, 15950–15963; d) S. V. Lindeman, S. V. Rosokha, D. L. Sun, J. K. Kochi, *J. Am. Chem. Soc.* **2002**, *124*, 843–855.
- [14] S. Hu, T. G. Spiro, *J. Am. Chem. Soc.* **1993**, *115*, 12029–12034.
- [15] Crystal data for *trans-2*-THF: triclinic, space group  $P\bar{1}$ ,  $a = 11.2481(11)$ ,  $b = 11.4296(11)$ ,  $c = 14.8280(14)$  Å,  $\alpha = 68.994(2)$ ,  $\beta = 79.051(2)$ ,  $\gamma = 81.188(2)^\circ$ ,  $V = 1739.7(3)$  Å<sup>3</sup>,  $Z = 1$ ,  $\rho_{\text{calc}} = 1.290$  mgm<sup>-3</sup>,  $T = 100(2)$  K, no. of reflections collected: 9362,  $\theta_{\text{max}} = 25.50^\circ$ ,  $R1 = 0.0552$  (for  $I > 2\sigma(I)$ ),  $wR2$  (all data) = 0.1311, goodness of fit on  $F^2$ : 1.052; largest diff. peak and hole: 0.472 and  $-0.318$  e Å<sup>-3</sup>. Crystal data for *trans-3*-I<sub>3</sub>: monoclinic, space group  $P2_1/c$ ,  $a = 16.3085(9)$ ,  $b = 19.1777(11)$ ,  $c = 15.0492(8)$  Å,  $\alpha = 90$ ,  $\beta = 107.0370(10)$ ,  $\gamma = 90^\circ$ ,  $V = 4500.2(4)$  Å<sup>3</sup>,  $Z = 2$ ,  $\rho_{\text{calc}} = 2.072$  mgm<sup>-3</sup>,  $T = 100(2)$  K, no. of reflections collected: 31223,  $\theta_{\text{max}} = 25.4991^\circ$ ,  $R1 = 0.0504$  (for  $I > 2\sigma(I)$ ),  $wR2$  (all data) = 0.1104, goodness of fit on  $F^2$ : 1.080; largest diff. peak and hole: 1.679 and  $-0.964$  e Å<sup>-3</sup>. CCDC1419602 (*trans-2*-THF) and 1419603 (*trans-3*-I<sub>3</sub>) contain the supplementary crystallographic data for this paper. These data can be obtained free of charge from The Cambridge Crystallographic Data Centre.
- [16] T. E. Clement, D. J. Nurco, K. M. Smith, *Inorg. Chem.* **1998**, *37*, 1150–1160.
- [17] a) M. Bröring, S. Köhler, C. Kleeberg, *Angew. Chem. Int. Ed.* **2008**, *47*, 5658–5660; *Angew. Chem.* **2008**, *120*, 5740–5743; b) S. Attar, A. L. Balch, P. M. Van Calcar, K. Winkler, *J. Am. Chem. Soc.* **1997**, *119*, 3317–3323; c) S. Attar, A. Ozarowski, P. M. Van Calcar, K. Winkler, A. L. Balch, *Chem. Commun.* **1997**, 1115–1116; d) D. Sahoo, S. P. Rath, *Chem. Commun.* **2015**, *51*, 16790–16793.
- [18] a) Y. Ni, S. Lee, B. B. Wayland, *Inorg. Chem.* **1999**, *38*, 3947–3949; b) S. Lee, M. Mediati, B. B. Wayland, *J. Chem. Soc. Chem. Commun.* **1994**, 2299–2300.
- [19] a) H. Song, R. D. Orosz, C. A. Reed, W. R. Scheidt, *Inorg. Chem.* **1990**, *29*, 4274–4282; b) H. Song, C. A. Reed, W. R. Scheidt, *J. Am. Chem. Soc.* **1989**, *111*, 6867–6868; c) K. E. Brancato-Buentello, W. R. Scheidt, *Angew. Chem. Int. Ed. Engl.* **1997**, *36*, 1456–1459; *Angew. Chem.* **1997**, *109*, 1608–1611.

Received: October 8, 2015

Published online: December 2, 2015